The self-assembly of self-interstitial-atoms caused by an electron beam

S. T. Nakagawa, K. Ohashi, and K. Sugita

Graduate School of Science, Okayama Univ. of Science, Japan.

1-1 Ridai-Cho Okayama 700-0005 Japan

Abstract:

A low energy electron beam (EB) can let the self-interstitial atoms (SIA) cause the self-assembly (DSA), i.e., {311}_{SIA} platelet in c-Si is discussed. We have studied how an SIA migrates toward metastable sites that form the platelet. We used a molecular dynamic (MD) simulation to trace all the atoms and crystallographic analysis method (PM) method to analyse crystalline defects. In MD, we skipped the EB irradiation stage that produces SIAs. Instead, before MD some Frenkel pairs (FP) or SIA coupled with a vacancy were randomly distributed in bulk. Then we monitored how contributed the surrounding target atoms to the DSA process. When the FP concentration is higher than 3 atomic percent (3 %), the number of atoms to be stayed at metastable sites looked to be saturated. However, it increased significantly at lower FP's concentration, e.g., at 1 %. At the same time, somewhat cooperative and oscillatory movement of target atoms in bulk was found in terms of the long-rangeorder (LRO) parameter. The oscillatory change of LRO continued for a few tens of ps, which is much slower than the so-called lattice vibration. Therefore, we suppose the cooperative motion like slow phonon might promote the migration of SIA and increase the number of atoms on {311}_{SIA} planes, whereas no such global wavy motion was observed in cases including much higher FPs, as if somewhat pinning effect had occurred therein.

Keywords; electron beam, MD simulation, directed self-assembly, crystallography

1. Introduction

The {311} platelet in a c-Si is known to be composed of the self-interstitial atom (SIA)s, which was found by the in-situ measurement using High Resolution Transmission Electron Microscopy by Takeda at an annealing temperature (T_A) of 723 K [Takeda (1991)]. This is a kind of directed self-assembly (DSA). Hereafter we call

(311)_{SIA} formation in c-Si DSA. The energy of the electron beam (EB) adopted was 300 keV, which was much higher than the threshold value of 145 keV to eject a target atom from a lattice site in c-Si. However, it was much lower than 1 MeV above which the electronic stopping is dominant [Yasuda et al. (2007)]. The very significant experimental condition to produce $\{311\}_{SIA}$ platelet was the T_A . The rate of fluence was $\Phi = 5 \times 10^{24}$ electrons/ sec/m² and it was continued for t = 1080 sec or longer. The procedure of DSA had two steps [Takeda and Kamino (1995)]; the first one was to form atomic rows along $\langle 0\bar{1}1\rangle$ direction, then the second one was to align those rows parallel along the direction of $\langle 2\bar{3}\bar{3}\rangle$, which formed (311) platelet. It was a notable experiment, because the geometry of this lattice structure was exactly the same with that predicted by the pixel mapping (PM) method; a (311)_{SIA} plane is made of *metastable* {H} or {T} sites [Nakagawa (2007a)].

Firstly, we had reproduced the DSA at $T_A = 723$ K using an ion beam (IB) (1keV Si ion into c-Si), making use of a molecular dynamic (MD) simulation [Nakagawa et al. (2007b)]. The two-step process of DSA that we found was exactly same with that proven by EB [Takeda and Kamino (1995)], and the areal density of the SIAs on (311)_{SIA} agreed with that experiment due to EB irradiation. The <110> alignment on (311)_{SIA} was clearly observed. The assignment of Miller index of an atomic plane or crystallographic orientation of an atomic row was possible using PM [Nakagawa et al. (2002; 2007a; 2009)]. This calculation proved that when SIAs are produced by whatever external disturbance, they migrate into the wide space between two sets of {311} double-layers and reallocated by the help of local field surrounding the SIA.

Secondly, assuming the Frenkel pair (FP) production due to EB irradiation, we had obtained quite similar result of DSA at $T_A = 723$ K, making use of a MD [Nakagawa (2014)]. Because the recoil cross-section of an electron against target atom is very small and it occurs so sparsely in a wide region. Then, we skipped the EB irradiation stage in MD. Instead we scattered FPs uniformly in bulk and then started MD to monitor the movement of all atoms. After heating started, SIAs migrated and formed a platelet, where <110> alignment was again observed.

A recent finding was the FP's concentration dependence on DSA. Target atoms in bulk showed somewhat cooperative and oscillatory behaviour of entire atoms, when the FP's concentration was lower than 3 atomic percent (3 %). The phonon-like motion was identified by the long-range-order (LRO) parameter that defined the degree of perfectness of crystallinity. In cases of higher FP's concentration, however,

no peculiar behaviour occurred, as if somewhat pinning-effect supressed the migration of SIAs. Present aim is to study how significantly the pinning-effect exerts on the DSA.

2. Method

2.1 Invisible but metastable sites for SIA

In the PM method, the location of an atom (x, y, z) in a cubic crystal is presented by a set of integer (l, m, n) using Gauss symbol [Nakagawa (2002)]. Namely, (l, m, n) = ([x/(d/4)], [y/(d/4)], [z/(d/4)]), where the "d" is the lattice constant of a unit cubic of a crystal. This means to adopt marginal space for each lattice site, and we call that small cube *one pixel*. The PM method is available for 24 cubic-type crystals belonging to the space group #195-#230.

The c-Si is one of the zincblende (ZnS)-type crystals, which is made of two fcc-(1) and fcc-(2) lattices. We regard a lattice point where one atom is occupies in a perfect crystal "stable site". These lattice points satisfy the following condition: In the fcc-(1) lattice, the address (l, m, n) of a stable site satisfies an algebraic rule of "l + m + n = 4k, and (l, m, n) are all even". Similarly, in the fcc-(2) lattice, the corresponding rule is "l + m + n = 4k + 3, and (l, m, n) are all odd". Both lattices are visible.

Table 1 The identification table for an atom located at (l, m, n) in a ZnS-type crystal, i.e., a compound AB. The last two planes are made of metastable $\{T\}$ and $\{H\}$, both form the *invisible double-layer structure*. "Meta." is the abbreviation of metastable.

" $(311)_{A'}$ or $(31)_{B'}$ means $\{311\}_{SIA}$. The "k" and "J" are arbitrary integers.

	Which site? Which crystal?			Which plane?		
Site	l+m+n	l, m, n	On which fcc lattice	D = 3l + m + n	Double-layer	Plane
(1)	4k	all even	real fcc-(1)	D=4J	Visible	{311} _A
Stable						
(2)	4k+3	all odd	real fcc-(2)	D=4J+1	Atoms at	{311} _B
Stable					lattice site	
{H}	4k+2	all even	virtual fcc-(1') from fcc-(1)	D=4J+2	Invisible	{311} _A ،
Meta.			shift by <2,0,0>		,	
{T}	4k+1	all odd	virtual fcc-(2') from fcc-(2)	D=4J+3	SIAs	{311} _B ,
Meta.			shift by <2,0,0>			

The PM makes it possible to identify various types of crystalline defects from micro to macroscopic scale. Another merit of the PM is to evaluate the LRO parameter [Nakagawa (2002, 2007a; 2009)], which is defined as the ratio of number of atoms allocated at stable sites to that of total atoms in the MD box. Note LRO = 1 means the state of a perfect crystal while LRO = 0 means amorphous state.

In Table 1, "metastable sites, {H} or {T}" are listed. They are closely related to the stable sites (1) and (2), respectively, although those lattices are invisible in a perfect crystal. The condition for {H} site is "l + m + n = 4k + 2, and (l, m, n) are all even". The similar condition for {T} site is "l + m + n = 4k + 1, and (l, m, n) are all odd". If the address of one atom does not satisfy any of those four conditions, the atom in a pixel for unstable site [Nakagawa (2002)].

Because of the translational symmetry between (1) and $\{H\}$, which are shifted by the constant vector of (0, 0, d/2) to each other, they individually form mathematically equivalent lattices with the same space group. The visible (1) and invisible $\{H\}$ are like twin lattices, although the former is stable and the latter is metastable. The situation is the same for (2) and $\{T\}$ [Nakagawa (2002)]. If some SIAs stay at such metastable sites, they look like a part of ZnS-type crystal and crystalline alignment as atomic row or atomic plane can be observed. Therefore, we have supposed, that invisible lattice can work as a hidden and secret chart for DSA. In this article, we examine the effect of the concentration of FPs on the DSA process, because the presence of embedded FPs should deform the potential field in bulk.

2.2 How to identify {311} defects;

A crystal has periodic array in a set of $\{HKL\}$ planes labelled by the fixed Miller index. When an atom has address (l, m, n) defined by PM, the sequential number of the (HKL) plane on which that atom stays is known as follows [Nakagawa (2009)],

$$D = l \times H + m \times K + n \times L \tag{1}.$$

When substituted the conditions for addresses of (1), (2), $\{T\}$, $\{H\}$, into Eq.(1) for a case of (HKL) = (311); we get an interesting correspondence. That is, stable site (1) and (2) are located on the planes termed D = 4J and D = 4J + 1, respectively. These two layers can form the visible paired double-layer. On the other hand, metastable $\{T\}$ and $\{H\}$ sites are on the planes termed D = 4J + 2 and 4J + 3, respectively. These two layers can form the *invisible paired double-layer*. This alignment is repeated every four layers as is tabulated in Table 1.

Making use of Table 1, we count how many SIAs are trapped at metastable sites, {H} or {T}, on the invisible {311}_{SIA} planes as will be plotted later in Fig. 2. The interplanar distance (ΔD) of adjacent plane in a series of $\{HKL\}$ planes is $d/\{H^2+K^2+L^2\}^{1/2}$. It is $\Delta D=d/\sqrt{11}$ for the case of {311} planes, thus the *invisible* paired double-layers yield wide gap of $3d/\sqrt{11}$ for an SIA between two sets of visible double-layers. A sheet of (311)_{SIA} plane has two dimensional diagonal grids made of $\langle 0\overline{1}1\rangle$ and $\langle 1\overline{2}\overline{1}\rangle$ axes. The area of one oblique unit cell of $11d^2$ is allocated to one metastable site on (311)_{SIA} plane. Since the shape of {311} planes inside the MD box are all polygons, because of truncation due to the surface of MD box adopted. When the MD box is composed of $p \times p \times p$ unit cubes, the address of the lattice point at the body-diagonal corner is (4p, 4p, 4p). Then as we look over the specific sites of (l, m, 4p). $n = (0, 0, 0) \rightarrow (2p, 2p, 2p) \rightarrow (4p, 4p, 4p)$, the D number of (311) plane including those sites changes from $D = 0 \rightarrow 10p \rightarrow 20p$. With increasing D-value, the number of metastable sites on those planes changes from zero -> maximum -> zero, respectively. Namely the number of metastable sites can show an upheaval profile as a function of D.

2.3 MD Simulation model

Generally speaking, the defect density in the collision cascade caused by an EB is much sparse if compared with the case due to an IB. With a low-energy EB below 1 MeV, the dominant energy loss is due to the nuclear stopping. The nuclear stopping power of 300 keV EB for silicon material is 2 eV/10 nm [Yasuda et al. (2007)]. Thus, one electron in an EB loses 1 eV when it penetrates a MD box whose depth is 5 nm. Namely, the depth doze of EB is very low. On the other hand with respect to the mean free path, the inelastic one is 240 nm while the elastic one is 12 nm. The formation energy of one FP is 3.61 eV. These facts make it possible to assume that the FPs would be distribution uniformly.

We embed FPs into c-Si prior to MD simulation. Here MD box is composed of $16 \times 16 \times 16$ unit cubes, thus 32768 silicon atoms are enclosed. With this box, D_{max} is 320. The range of FP's concentration is from 1 % to 10 %. We adopted the so-called NVT frame for our MD, where three quantities are kept constant; they are the number (N) of target atoms, the volumn (V) of the MD box, and the bulk temperature (T). After distributing FPs, we started MD simulation in the following order: (i) Thermalization to keep T constant at room temperature (T = 300K; RT). When the deviation of (T-RT)/T is stabilized within the fluctuation less than 1.0 % in average, next step started. (ii) Heating up to T_A . At MD box walls, particle's velocity was regulated to yield the

heating rate of 0.5 K/femtosecond. When the deviation $(T-T_A)/T$ becomes less than 1.0 %, further heating was quitted. (iii) Annealing to keep $T = T_A$ for 200 picoseconds (ps) at longest.

3. Result

3.1 How SIA migrates towards metastable site?

Figure 1 shows the change in the fractions of atoms staying different sites, after starting heating (time t = 0) for a case of 3 % of FP's concentration, where $T_A = 1000$ K. Symbols indicate the ratios of atoms located at stable (-), metastable (\circ), unstable (--) sites to the number of total atoms.

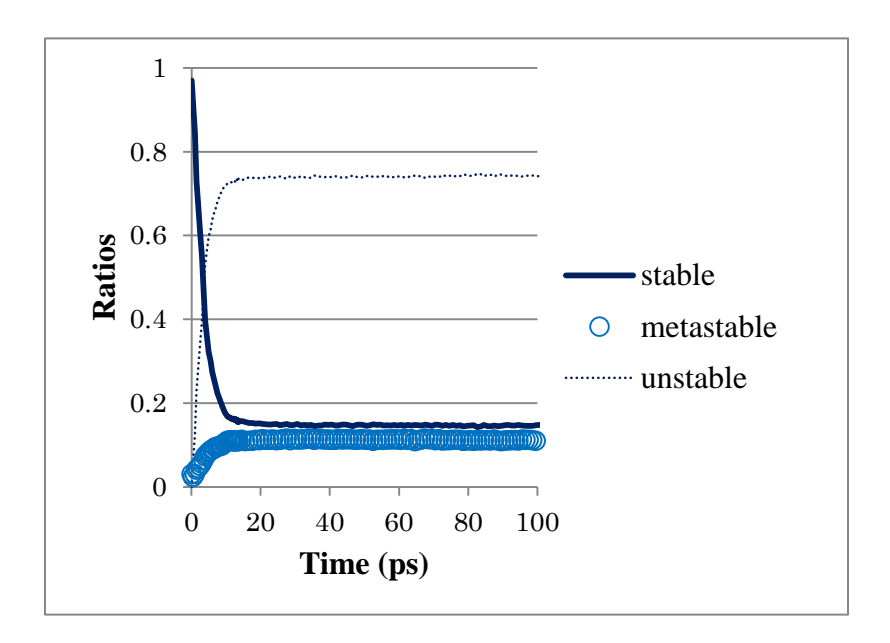


Figure 1 Time series of the site distribution of target atoms, since starting heating from RT to $T_A = 1000$ K, for a case with 3 % of FP concentration. Symbols indicate the ratios of atoms located at stable (-), metastable (\circ), unstable (--) sites.

From this figure, it is known that many atoms left the original stable site within 10 ps after heating started, which was crystal to amorphous (CA) transition. Since then, it looks no significant change in those fractions of three kinds of states after CA transition. In the case of of higher concentration, 5 % and 10 %, such situation was quite similar, there was no significant concentration dependence. In the mean time,

the number of atoms at metastable sites, {T} or {H}, increased significantly and reached at the same level with that at stable sites here.

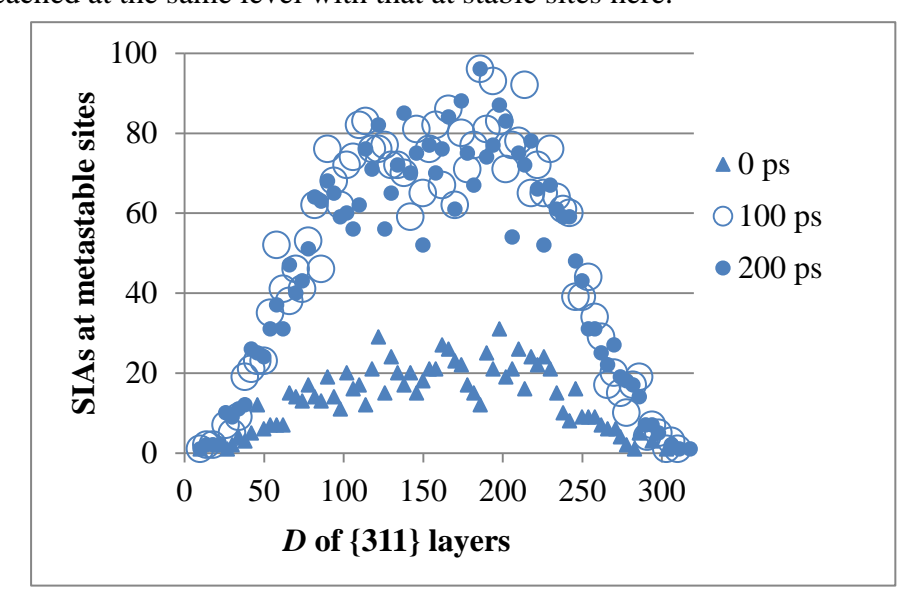


Figure 2 The time dependence of the SIA accumulation toward metastable sites on $(311)_{SIA}$, where $T = T_A = 1000$ K is kept. Each symbol indicates the sum of atoms leated at metastable sites on one paired invisible double-layers.

Figure 2 shows the significant accumulation of atoms toward metastable sites due to heating up to $T_A = 1000$ K when FP's concentration is 3 %. The migration was promoted evidently until 100 ps. However, since then any further migration toward metastable sites looked supressed. Even increasing FP's concentration, up to 10 %, migration looks less easy as if somewhat pinning-effect might have appeared.

3.2 The pinning-effect on the DSA

Figure 3 shows the FP's concentration dependence on the number of atoms trapped at metastable sites. The number of atoms located at metastable sites did not increase with the initial FP's concentration but showed rather saturation when the initial concentration was higher than 3 %. The migration of SIAs can be assisted by atoms nearby. Therefore, we will examine why such concentration dependence happened. The movement of target atoms can be monitored in terms of the LRO parameter. Note *LRO* is equal to the ratio of occupied number of atoms at stable sites to that of the total atoms as was plotted in Fig. 1

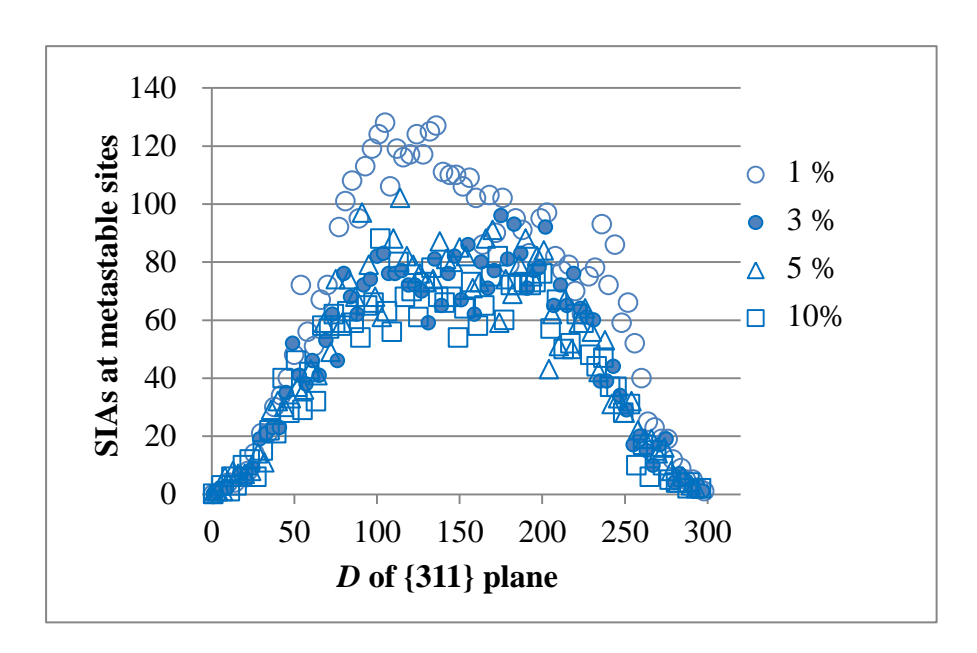


Figure 3 The FP's concentration dependence on the SIA migration toward the metastable sites within 100 ps at $T_A = 1000$ K. Symbols for different concentrations are (\circ ; 1%), (\bullet ; 3%), (Δ ; 5%), and (\square ; 10%).

3.3 The cooperative motion of target atoms vs. the pinning effect:

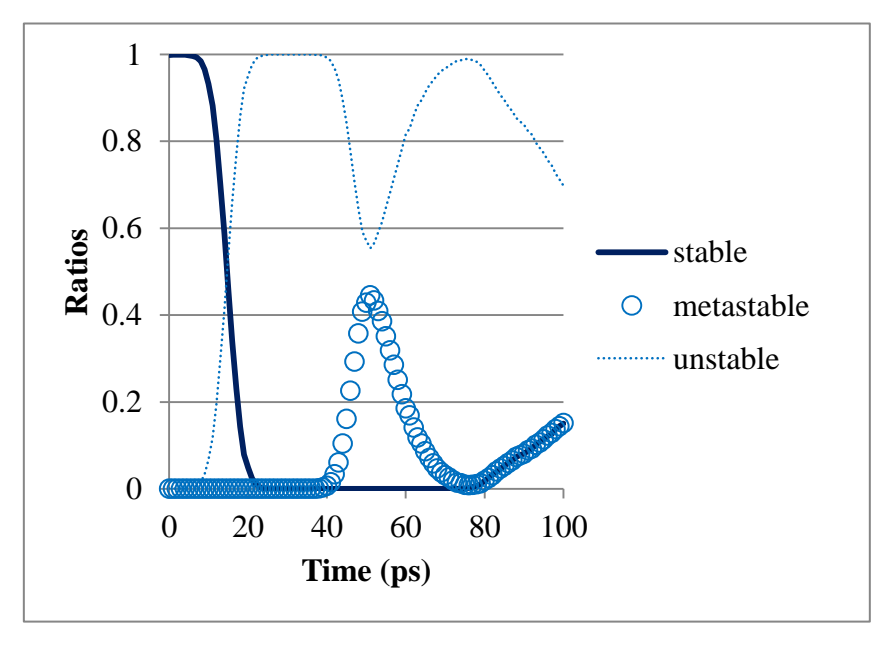


Figure 4 Time series of the site distribution when the initial concentration of FP was 1 % with keeping T_A = 1000 K. Notations are same to Fig. 1.

If compared this Fig.4 with Fig.1, the presence of somewhat global and synagistic movemnet of target atoms is evident when FP concentration is low. Moreover the

trend of restoration of LRO looked, at around 50 ps and after 80 ps, although there was once disappeared by the slower CA transition if compared with Fig.1. This oscillatory and cooperative motion of atoms located at metastable sites inversely corresponds to that at unstable ones, which implies the simultaneous migration of many SIAs. This result could explain the profile of Fig. 3; more atoms were located at metastable sites when less FPs were scattered before MD. The increasing ratios of stable and metastable after 80 ps indicate the sign of further restoration by the assist of deformed potential field. In other words, the presence of much FPs may cause like pinning-effect that may suppress such a cooperative motion of target atoms as was shown in Fig.1

4. Conclusion

We have studied why the SIA is apt to form the $\{311\}$ planar defect (= $(311)_{SIA}$ platelet) in c-Si when it was irradiated by a low-energy (sub-MeV) EB or a low energy (a few keV or less) IB. We traced all the atoms by an empirical MD simulation, and analysed the crystalline defects by the PM method.

Based on the PM, we have supposed the DSA is directed by the hidden chart for migrating SIAs. Because the measured DSA had shown exactly same geometrical lattice structure with that described by the PM method. That is, metastable sites are forming hidden fcc lattices in the wide gap between two sets of {311} double-layers. Therefore, when an SIA would migrate, it is apt to enter such wide space and would be trapped at metastable sites, where the hidden lattice would provide a chart for migrating SIA.

The EB irradiation first produces many FPs in c-Si. Then we embedded FPs and started MD simulation to monitor how target atoms assist SIAs to migrate and form the {311}_{SIA} platelet, in terms of the long-range-order parameter. We have confirmed that a global and synergistic movement of target atoms promoted the migration of SIAs, when the FPs concentration is lower than three atomic percent. Beyond the critical value of 3 %, however, pinning effect emerged, i.e., no significant cooperative wavy-motions occurred, and the defect formation is suppressed.

Acknowledgment

This work has been supported by a grant for Scientific Research (C) (Grant No. 21510108) from JSPS (Japan Society for the Promotion of Science) and partly by a grant for Scientific Research on Innovative Areas (Grant No. 21104003) from MEXT (Ministry of Education, Culture, Sports, Science, and Technology, Japan) and partly supported.

References

- Takeda, S. (1991), An Atomic Model of Electron-Irradiation-Induced Defects on {113} in Si, *Jpn. J. Appl. Phys*, **30**, L639-642.
- Takeda, S.; Kamino, T. (1995), Agglomeration of self-interstitials in Si observed at 450 °C by high-resolution transmission electron microscopy, *Phys. Rev. B*, **51**, 2148-2152.
- Nakagawa, S. T. (2002), Pixel mapping analysis to characterize long-range order interactions in crystals under ion irradiation, *Phys. Rev. B*, **66**, 094103/1-7.
- Nakagawa, S. T. (2007a), Crystallographic analysis of phase-changes in cubic crystals, *J. Phys. Soc. Jpn.*, **76**, 034603/1-12.
- Nakagawa, S. T.; Whitlow H. J.; Betz, G. (2007b), Detection of planar defects caused by ion irradiation in Si using molecular dynamics, *Surf. Coating Tech.*, **201**, 8393-8397.
- Nakagawa, S. T. (2009), In Ion beams in Nanoscience and Technology (Chap.9), Springer
- Nakagawa, S. T. (2014), The directed self-assembly for the surface pattering by electron beam, *Rad. Effect Defect Solids*, (2014) doi: 10.10 80/10420150.2014.984613.
- Yasuda, M.; Kimoto, Y.; Tada, K.; Mori, H.; Akita, S.; Nakayama, Y.; Hirai, Y. (2007), Molecular dynamics study of electron-irradiation effects in single-walled carbon nanotubes, *Phys. Rev. B*, **75**, 205406/1-5.